AMERICAN SOCIETY FOR MICROBIOLOGY | Molecular and Cellular Biology

MicroRNA 140 Promotes Expression of Long Noncoding RNA NEAT1 in Adipogenesis

Ramkishore Gernapudi,[a] Benjamin Wolfson,[a] Yongshu Zhang,[a] Yuan Yao,[a] Peixin Yang,[b] Hiroshi Asahara,[c,d] Qun Zhou[a]

Department of Biochemistry and Molecular Biology, Greenebaum Cancer Center, University of Maryland School of Medicine, Baltimore, Maryland, USA[a]; Department of Obstetrics, Gynecology and Reproductive Sciences at University of Maryland School of Medicine, Baltimore, Maryland, USA[b]; The Scripps Research Institute Department of Molecular and Experimental Medicine, La Jolla, California, USA[c]; Department of Systems Biomedicine, Tokyo Medical and Dental University, Bunkyo-ku, Tokyo, Japan[d]

More than 40% of the U.S. population are clinically obese and suffer from metabolic syndrome with an increased risk of postmenopausal estrogen receptor-positive breast cancer. Adipocytes are the primary component of adipose tissue and are formed through adipogenesis from precursor mesenchymal stem cells. While the major molecular pathways of adipogenesis are understood, little is known about the noncoding RNA signaling networks involved in adipogenesis. Using adipocyte-derived stem cells (ADSCs) isolated from wild-type and microRNA 140 (miR-140) knockout mice, we identify a novel miR-140/long noncoding RNA (lncRNA) NEAT1 signaling network necessary for adipogenesis. miR-140 knockout ADSCs have dramatically decreased adipogenic capabilities associated with downregulation of NEAT1 expression. We identified a miR-140 binding site in NEAT1 and found that mature miR-140 in the nucleus can physically interact with NEAT1, leading to increased NEAT1 expression. We demonstrated that reexpression of NEAT1 in miR-140 knockout ADSCs is sufficient to restore their ability to undergo differentiation. Our results reveal an exciting new noncoding RNA signaling network that regulates adipogenesis and that is a potential new target in the prevention or treatment of obesity.

More than 40% of American adults are overweight or obese, and there are over 40 million obese women in America (1). Obese and overweight women are at greater risk for postmenopausal breast cancer and have dramatically higher rates of cancer recurrence and mortality (2, 3). Obesity is characterized by metabolic imbalance leading to adipocyte hypertrophy and hyperplasia and the excess accumulation of adipose tissue. During adipogenesis, mesenchymal stem cells (MSC) commit to the adipogenic lineage, forming proliferative, MSC-like cells called preadipocytes. By differentiating into mature adipocytes, preadipocytes replenish the nonproliferative mature adipocytes that are the bulk of white adipose tissue (4). Mature adipocytes secrete hormones and adipokines that, in addition to their metabolic function, promote breast tumor aggressiveness and invasion (5). Deciphering the mechanisms of preadipocyte differentiation and adipocyte-breast cancer cell interaction will greatly further our understanding of and our ability to treat breast cancers.

MicroRNAs (miRNAs) are essential regulators of cellular function and gene expression. After nuclear processing, miRNA precursors are exported to the cytoplasm, where the mature miRNA is formed. miRNAs associate with the RNA-induced silencing complex (RISC) and base pair to seed sequences in the 3′ untranslated region (UTR) of target mRNAs. This guides the RISC to the mRNA, causing degradation or inhibition of translation. miRNAs primarily function in the cytoplasm; however, some have been shown to translocate back into the nucleus and degrade nuclear RNA molecules (6). Nuclear miRNAs have also been shown to mediate mRNA upregulation by RNA activation (RNAa). This occurs through the direct binding of an miRNA to the gene promoter and recruitment of Argonaute proteins. The miRNA-Argonaute complex recruits histone methyltransferase proteins, leading to epigenetically active chromatin and increased transcriptional activity (7). Alternatively, miRNAs targeting the 3′-terminal region have been shown to activate transcription, potentially through the formation of a loop that brings the 3′ terminus close to the promoter and recruits activating proteins. miRNAs that target enhancer sequences within the gene may have similar transcription-activating effects (8). miRNAs have also been shown to increase mRNA expression by competitively binding AU-rich regions in the 3′ UTR, preventing degradation by RNA binding proteins (9).

miRNAs have been extensively studied in cancer and regulate various physiological processes at the posttranscriptional level (10). Several miRNAs have been found to play important regulatory roles in either promoting (miR-140, miR-26a/b, and miR-455) (11, 12) or suppressing (miR-27 and miR-133) adipogenesis (13, 14). miR-140 is an important regulator of developmental pathways and stem cell differentiation and is a tumor suppressor in breast cancer (15–17). Through targeted degradation of the stem cell factors SRY (sex-determining region Y) box 2 (SOX2), SOX9, and ALDH1, miR-140 prevents breast cancer initiation and progression. Expression of miR-140 is downregulated in estrogen receptor-positive breast cancers due to estrogen-mediated transcriptional inhibition, while epigenetic mechanisms of inhibition have been demonstrated in basal-like breast cancers (16, 18). Decreased miR-140 expression releases suppression of breast cancer stem cells, leading to higher tumorigenicity. Recent work has identified a role of miR-140 in adipogenesis. In pluripotent stem cells, miR-140 is activated by bone morphogenic protein 4 (BMP4) and induces commitment to the adipogenic lineage by

Received 14 July 2015 **Returned for modification** 15 August 2015
Accepted 2 October 2015

Accepted manuscript posted online 12 October 2015

Citation Gernapudi R, Wolfson B, Zhang Y, Yao Y, Yang P, Asahara H, Zhou Q. 2016. MicroRNA 140 promotes expression of long noncoding RNA NEAT1 in adipogenesis. Mol Cell Biol 36:30–38. doi:10.1128/MCB.00702-15.

Address correspondence to Qun Zhou, qzhou@som.umaryland.edu.

R.G. and B.W. contributed equally to this article.

targeting the adipogenesis inhibitor osteopetrosis-associated transmembrane protein 1 (OSTM1) for degradation (19).

Long noncoding RNAs (lncRNAs) (>200 bp) are one of the most abundant types of noncoding RNA and have vital roles in differentiation and tissue homeostasis. Sun et al. identified several lncRNAs that are dramatically upregulated during adipogenesis, including NEAT1 (13). NEAT1 is a nuclear lncRNA that is a necessary scaffolding factor for the formation of nuclear paraspeckles. Paraspeckles are nuclear bodies comprised of a NEAT1 backbone that interacts with core paraspeckle proteins, including polypyrimidine tract-binding protein-associated splicing factor (PSF), 54-kDa nuclear RNA binding protein (p54nrb), and polymerase suppressor protein 1 (PSP1) (20). These and other paraspeckle proteins sequester certain mRNA transcripts at the paraspeckle and mediate posttranscriptional splicing. While NEAT1 paraspeckles are necessary for myeloid differentiation and play a key role in mammary gland development and lactation (21), the functions of paraspeckles are still largely unknown (22).

The paraspeckle-independent functions of NEAT1 are mostly uncharacterized. However, NEAT1 has been shown to localize to epigenetically active chromatin and may be an important activator of gene transcription (23, 24).

Interaction between noncoding RNA molecules is a novel and likely crucial regulatory mechanism within the cell. The best-characterized mechanism of lncRNA-miRNA interaction is by competitive endogenous lncRNAs. One example of this is lncRNA-regulator of reprogramming (RoR), which contains several miR-145 binding sites. lncRNA-RoR acts as a competitive sponge for miR-145, increasing expression of other miR-145 targets. This is a mechanism for maintaining self-renewal signaling in human embryonic stem cells, triple-negative breast cancer, and endometrial tumor spheres (25–27). miRNAs can also regulate lncRNAs by targeting them for degradation via the RNA-induced silencing complex (28). While miRNA-mediated degradation was previously believed to be restricted to the cytoplasm, miRNAs and RISC proteins were recently found to be present in the nucleus and are able to degrade lncRNAs that are restricted to the nucleus (6).

Here, we demonstrate the critical role of miR-140 in preadipocyte differentiation and identify NEAT1 as a novel downstream target of miR-140 in adipogenesis. We report the first instance of nuclear localization of miR-140, where it physically interacts with NEAT1 and enhances the expression of NEAT1. Through the use of wild-type (WT) and miR-140 knockout (KO) primary mouse preadipocytes, we show that miR-140 knockout results in downregulation of NEAT1, abrogating the preadipocyte adipogenic ability. Reexpression of NEAT1 in miR-140 knockout mouse primary preadipocytes restores the adipogenic phenotype, showing regulation of NEAT1 expression is a primary function of miR-140 in adipogenesis.

MATERIALS AND METHODS

Cell culture, reagents, transfection, and actinomycin D. MCF10DCIS (DCIS) breast cancer cells obtained from Asterand (Detroit, MI) and murine 3T3-L1 preadipocytes and human lung fibroblasts obtained from the ATCC were cultured as previously described (17, 29). Human mammary preadipocytes (mammary adipocyte precursor cells) were purchased from ZenBio (Research Triangle Park, NC) and were maintained and differentiated as described previously (30). The cells were incubated in 5% CO_2 at 37°C. Sulforaphane (SFN) purchased from LKT laboratories (St. Paul, MN) was used at 5 μM and 10 μM concentrations for all assays. The sulforaphane was dissolved in ethyl alcohol (EtOH). All transfection assays were performed as described previously by Li et al. (16). For actinomycin D RNA stability, cells were grown to ~50% confluence and treated with 10 μg/ml actinomycin D (Sigma) in dimethyl sulfoxide (DMSO). Control cells were treated with DMSO.

Adipose tissue stromal vascular fraction and differentiation assays. The adipose tissue stromal vascular fraction (SVF) was isolated from the fat tissue of 10- to 12-week-old WT and miR-140 KO mice as previously described (15, 31). The fat tissue (1.5 to 2.0 g) was cut up and digested with collagenase at 37°C for 1 h with spinning once every 15 min. After digestion, the solution was filtered through 250-μm tissue strainers (Thermo Scientific, Rockford, IL) and collected in a sterile tube. After centrifugation at 200 × *g*, the filtrate was comprised of mature adipocytes (top layer) and the SVF (bottom layer). The pellet (SVF) was washed twice with phosphate-buffered saline (PBS) and resuspended in culture medium (Dulbecco's modified Eagle's medium [DMEM], 10% fetal bovine serum [FBS], 1% penicillin-streptomycin). The cell solution was filtered through a 40-μm cell strainer and transferred to a 10-cm tissue culture dish. For *in vitro* differentiation assays, the cells were treated with an adipogenic cocktail containing 0.5 mM 3-isobutyl-1-methylxanthine (IBMX), 1 μM dexamethasone, 8 μg/ml biotin, 1 μg/ml bovine insulin, and 10% fetal bovine serum. The differentiated adipocytes were maintained in medium containing 10% FBS supplemented with 1 μg/ml insulin and 8 μg/ml biotin. Animal studies complied with federal guidelines and institutional policies of the University of Maryland Animal Care and Use Committee.

Oil Red O staining. Adipocytes were washed twice with PBS and fixed in 10% formalin at room temperature for 30 min. Oil Red O working solution was prepared and freshly filtered prior to the staining. After fixation, the cells were exposed to 60% isopropyl alcohol and allowed to dry completely at room temperature. The cells were stained with Oil Red O for 30 min at room temperature. The stained intracellular lipid droplets were washed twice with distilled water (dH_2O) and visualized with a Nikon Eclipse Ti-U microscope. Quantification was performed using ImageJ analysis.

Sphere formation assay. Cells were separated using cell dissociation buffer (Millipore) and 40-μm strainers (Fisher Scientific, Pittsburgh, PA). A total of 20,000 cells/ml were seeded in six-well plates coated with 2% polyhema (Sigma). After 7 days, spheres of >100 μm were quantified.

NEAT1 cloning. Mouse Neat1 was amplified by PCR using the genomic DNA of NIH 3T3-L1 cells as a template with the primers 5′-ACTGATGCCGGCAGGAGTTAGTGACAAGGAGGG-3′ and 5′-ACTGATGTCGACGAAGCTTCAATCTCAAACCTTTA-3′ and cloned into the NgoMIV and SalI sites of the pBABE-puro vector. The pZw1-sno vector was digested with HindIII, treated with T4 DNA polymerase, and then digested with SalI. The pBABE-mNeat1 vector was digested with NgoMIV, treated with T4 DNA polymerase, and digested with SalI. Neat1 was then recovered and cloned into the pZw1-sno vector (32).

Biotinylated-probe pulldown. Pulldown of miR-140 targets was performed as described previously (33). Binding of miR-140 to NEAT1 was tested using biotin-labeled miR-140. Briefly, 3T3-L1 cells were transiently transfected with a miR-140 duplex in which biotin was attached to the 3′ end of the sense strand. After 24 h, whole-cell lysates were prepared and mixed with streptavidin magnetic beads (New England Biolabs) and incubated with rotation at 4°C for 16 h. The beads were then collected and washed thoroughly. The bead-bound RNA was extracted, treated with DNase, and purified for further analysis. The levels of specific RNAs were measured by quantitative real-time (qRT) PCR. As a control, input RNA was also prepared.

qRT-PCR. qRT-PCR analysis of mRNA/miRNA/lncRNA expression was performed as described previously with normalization to either GAPDH (glyceraldehyde-3-phosphate dehydrogenase) or β-actin for mRNAs and to U6 small nuclear RNA for miRNAs.

Immunofluorescence. Cells were fixed with 4% paraformaldehyde for 10 min, washed twice with PBS, and blocked with 10% goat serum in PBS at room temperature for 1 h, followed by primary-antibody

(1:250) incubation overnight at 4°C. After incubation with secondary antibody for 1 h, followed by washes in PBS and counterstaining with DAPI (4′,6-diamidino-2-phenylindole) in PBS for 10 min at room temperature, samples were mounted using mounting medium (KPL, Gaithersburg, MD) and visualized with an Olympus IX81 spinning-disk confocal microscope. Quantification was performed using ImageJ analysis.

Immunohistochemistry (IHC). Paraffin-embedded tissue sections were deparaffinized in xylene, rehydrated in ethanol, and washed twice with dH_2O. Antigen retrieval was performed using 10 mM sodium citrate, pH 6.0, at 95°C for 10 min with cooling for 30 min at room temperature. Samples were quenched using 3% hydrogen peroxide, followed by washing and blocking with 10% goat serum in PBS. The samples were incubated with the primary antibody overnight at 4°C in antibody diluent, washed, and incubated with secondary antibody for 1 h at room temperature. The substrate reaction was performed using the DAB horseradish peroxidase (HRP) substrate (Vector Laboratories, CA) for peroxidase. Sections were mounted using DPX (Sigma, USA) and visualized using a Nikon Eclipse Ti-U microscope.

Fluorescence *in situ* hybridization (FISH). miRNA and lncRNAs were studied using the methodology previously described with necessary modifications (26, 34). Fluorescein isothiocyanate (FITC)-labeled lncNEAT1 probe was obtained from Affymetrix. Briefly, cells were fixed with 4% paraformaldehyde and treated with proteinase K, which helps to expose the cellular RNA to the probe. After 5 min incubation in permeabilization buffer (0.5% Triton X-100 in 1× PBS), samples were blocked in prehybridization buffer (3% bovine serum albumin [BSA] in 4× SSC [1× SSC is 0.15 M NaCl plus 0.015 M sodium citrate]) for 30 min at 55°C and incubated in hybridization buffer (4× SSC plus 10% dextran sulfate) with probe diluted at 1:5,000 for 2 h at 55°C. After brief washing in different grades of wash buffers (I, II, and III) and peroxidase treatments, samples were blocked (4% BSA in 1× PBS) for 1 h at room temperature, followed by primary-antibody incubation overnight at 4°C. The samples were washed in PBS and incubated in secondary antibody for 1 h, followed by DAPI for 10 min in the dark at room temperature. Slides were mounted using mounting medium (KPL, Gaithersburg, MD) and visualized with an Olympus IX81 spinning-disk confocal microscope. All the buffers in the above-described experiments were freshly prepared on the day of the experiment.

Plasmid constructs and luciferase assay. The miR-140 targeting sites within the mouse Neat1 sequence were established using RNAhybrid 2.2, a tool for finding minimum free energy hybridization (http://bibiserv.techfak.uni-bielefeld.de/rnahybrid) (39). The first Neat1 fragment, containing a putative miR-1403p targeting site, was amplified by PCR using a pair of primers, 5′-ACGTTTGCTAGCTTCCGTGCTTCCTCTTCTGT-3′ (forward) and 5′-ACGTTTCTCGAGTTCACTGTGTAGGCGTCAAC-3′ (reverse), and cloned into the NheI and XhoI sites of the pSGG vector. This constructed reporter was named pSGG-miR140-BS1. The second Neat1 fragment, which contained a putative miR-140 targeting site, was amplified by PCR using the primers 5′-ACGTTTGCTAGCACCGTGGGTTGATGGGAATA-3′ (forward) and 5′-ACGTTTCTCGAGGAAGGCATGGCTCACACATT-3′ (reverse) and cloned into the pSGG vector. The second constructed reporter was named pSGG-miR140-BS2. To construct the mutant reporter plasmid, we used the Generate site-directed mutagenesis system (Invitrogen) to introduce mutations into the putative miR-140 targeting sites of the pSGG-miR140-BS1 vector. The primers used for the mutant reporter construction were 5′-GTGACCGGAAACATCGATGTGAGCCCTCGCAAGGCTCCACACTCACGTC-3′ and 5′-GACGTGAGTGTGGAGCCTTGCGAGGGCTCACATCGATGTTTCCGGTCAC-3′. The constructed mutant reporter plasmid containing six point mutations, TGGA(C to G)CCT(G to T)G(G to C)G(T to A)GGGCTCACA(G to T)C(C to G)ATGT, was confirmed by sequencing. Luciferase reporter transfection and dual-luciferase assays were performed as described previously (35).

Statistical analysis. Statistical analysis was performed by Student's *t* test. *P* values of <0.05 were considered significant. Data are presented as means and standard errors (SE). Data were analyzed using GraphPad Prism software (version 6.0).

RESULTS

miR-140 is required for adipogenesis. The adipose tissue SVF is capable of proliferating and differentiating into several lineages, including adipocytes. These adipocyte-derived stem cells (ADSCs) have been used to characterize signaling pathways that are required for adipogenesis in both mice and humans (36). To determine if miR-140 is necessary for adipogenic commitment, we isolated adipose tissue SVF from WT and miR-140 KO mice. We incubated the SVF of WT and miR-140 KO adipose tissue for 10 days in adipocyte differentiation medium and quantified the mature adipocytes using Oil Red O lipid droplet staining. As seen in Fig. 1A and B, differentiation of miR-140 KO SVF was dramatically reduced compared to WT SVF. Western blotting for peroxisome proliferator-activated receptor γ (PPARγ) and C/EBPα, two key transcription factors that are the primary drivers of adipogenesis and are common markers of mature adipocytes, found less protein expression in miR-140 KO adipocytes, confirming a decrease in their adipogenic ability (Fig. 1D). Adipose tissue SVF (adipocyte-derived stem cells) is composed of multiple cell types, including white adipocyte progenitor cells or preadipocytes (4). To verify the physiological similarity of adipocyte-derived stem cells to the 3T3-L1 cell model, we treated both WT and miR-140 KO SVF with SFN, a compound previously shown to inhibit adipogenesis in mouse 3T3-L1 preadipocytes (30). As previously reported, preadipocyte differentiation was decreased in a dose-dependent manner (Fig. 1A and B) in both WT and miR-140 KO cells, verifying our successful isolation of primary mouse adipocyte-derived stem cells. Using immunofluorescence staining for PPARγ and C/EBPα, we confirmed that SFN decreases PPARγ and C/EBPα expression in miR-140 KO cells (Fig. 1E and F). Because mature adipocytes are the primary component of adipose tissue and the mammary gland and have been shown to enhance breast cancer cell invasion and aggressiveness (5), we investigated the effect of miR-140 KO on *in vivo* mammary adipose tissue. Using IHC, we examined the expression of the mature adipocyte markers C/EBPα, PPARγ, and adiponectin in the adipose tissue from WT and miR-140 KO mammary glands and found that all three mature adipocyte markers were considerably downregulated in adipocytes within miR-140 KO mammary tissue. This demonstrates that miR-140 deficiency leads to an inhibitory effect on adipogenesis within the mammary gland (Fig. 1C).

NEAT1 is upregulated in mature adipocytes. As we found that miR-140 is required for adipogenesis, we next wanted to examine the molecular mechanism of miR-140 action and to identify miR-140 targets important for adipogenesis. Recent work by Sun et al. profiled the transcriptomes of mouse preadipocytes and differentiated adipocytes and found several lncRNAs that are strongly and specifically regulated during adipogenesis (13). Because miR-140 knockdown prevents adipogenesis, we hypothesized that one mechanism of miR-140 action during adipogenesis is to regulate lncRNA expression. First, we profiled the alterations in lncRNA expression during human preadipocyte adipogenesis. Using a noncoding RNA qPCR array (System Biosciences), we compared the expression of 90 lncRNAs with well-known roles in transcriptional control and epigenetic regulation in primary human adipocyte-derived stem cells to expression in differentiated adipocytes. Analysis of the array revealed that 41 out of the 90 lncRNAs profiled had at least a 1.5-fold change in expression in mature adipocytes compared to adipocyte-derived stem cells (3

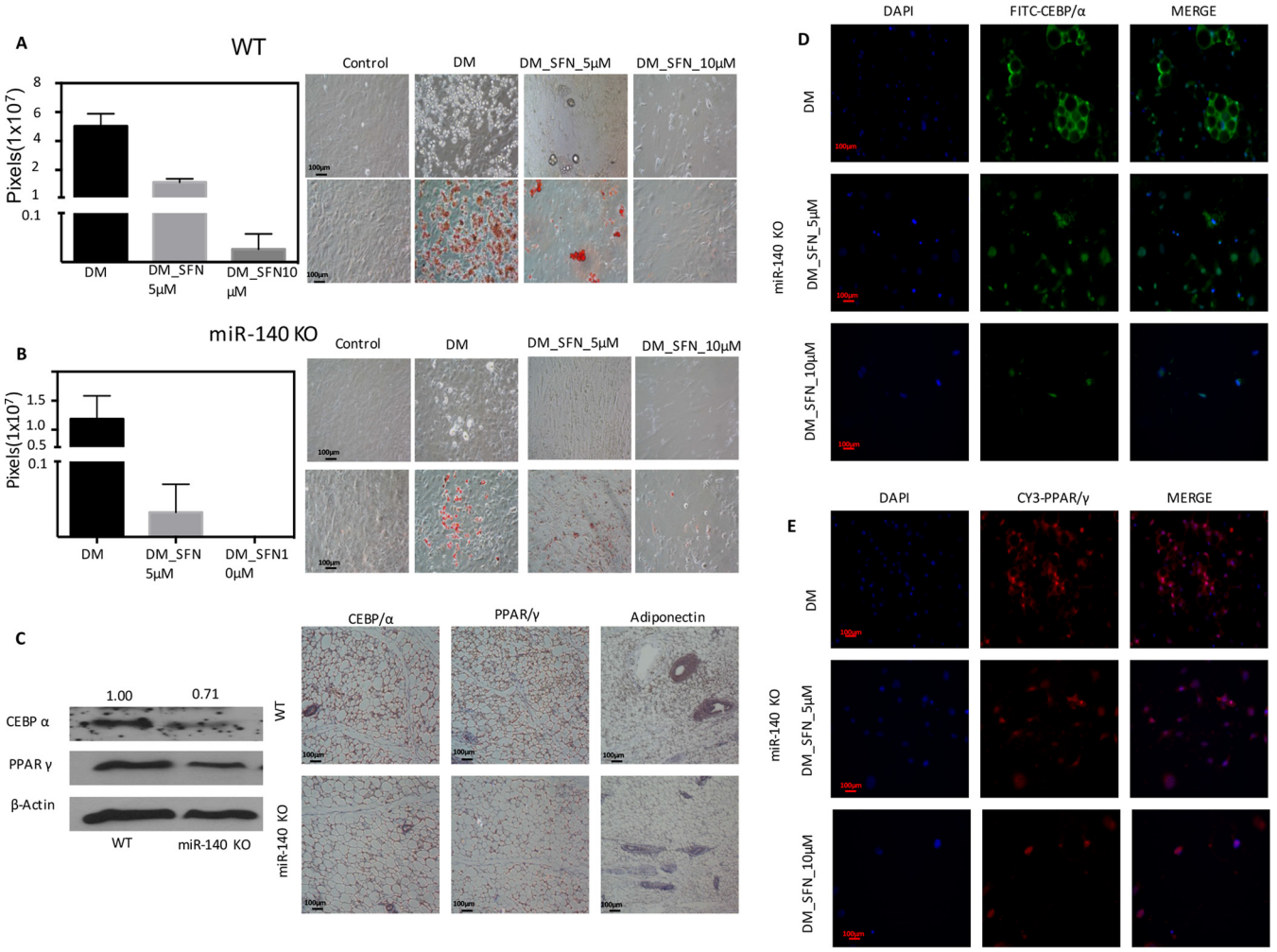

FIG 1 SFN treatment inhibits preadipocyte differentiation in primary SVF. (A) Sulforaphane treatment (5 or 10 μM) resulted in a dramatic decrease in differentiation, as evidenced by a decrease in lipid droplet accumulation. Primary SVF following differentiation (the 9th day after stimulation with D-biotin, dexamethasone, insulin, and IBMX cocktail) was stained with Oil Red O. (B) Primary SVF obtained from miR-140 KO mice showed a decrease in differentiation in both the presence and absence of SFN (5 or 10 μM). Oil Red O staining indicated that the knockout of miR-140 resulted in a decrease in differentiation, and SFN treatment (5 or 10 μM) blocked adipocyte differentiation. (C) Protein analysis of differentiated WT and miR-140 KO adipocytes for adipocyte markers CEBP/α and PPARγ and IHC imaging of mammary tissue sections from WT and miR-140 KO mice for adipocyte markers, CEBP/α, PPARγ, and adiponectin. Brown precipitate was developed using an avidin-biotin peroxidase substrate kit (Vector Laboratories, CA). Nuclei were counterstained with hematoxylin. The images were captured using a Nikon-Ti microscope. (D and E) Immunofluorescence imaging of differentiated adipocytes. The SVF from miR-140 KO was allowed to differentiate in an adipogenic cocktail with or without SFN (5 or 10 μM) for 10 days. After differentiation, cells were fixed in 4% paraformaldehyde (PFA) and analyzed for the expression levels of mature adipocyte markers (CEBP/α and PPARγ). The cells were stained with anti-rabbit Alexa 488- or 555-conjugated secondary antibody, and nuclei were counterstained with DAPI. Shown are representative images from experiments done in triplicate. The scale bars represent 100 μm. The data represent means and SE.

downregulated and 38 upregulated). As seen in Fig. 2A, of the lncRNAs examined, seven were increased at least 4-fold, including NEAT1. This shows that NEAT1 is upregulated in human adipocyte-derived stem cells during adipogenesis, confirming the previously reported findings in mouse preadipocytes (13) (Fig. 2A). NEAT1 is highly conserved between humans and mice, and while several studies have demonstrated NEAT1 function in paraspeckle formation, little work has been done to define the physiological functions of NEAT1. Therefore, we chose to explore the role of NEAT1 in adipogenesis. To confirm our array data, we used real-time qRT-PCR to compare the level of NEAT1 expression in primary human adipocyte-derived stem cells to that in differentiated adipocytes. We also examined NEAT1 expression in human lung fibroblasts and MCF10DCIS breast cancer cells to determine whether NEAT1 upregulation is specific to adipocytes. NEAT1 was enriched in adipocyte-derived stem cells over other cell lines and was increased 6.5-fold in differentiated adipocytes compared to adipocyte-derived stem cells. This demonstrates that NEAT1 is expressed at higher levels in cells committed to the adipogenic lineage and that NEAT1 is highly induced during adipogenesis (Fig. 2B). Finally, we used qRT-PCR to compare the expression of NEAT1 and three other lncRNAs in primary human adipocyte-derived stem cells to that in differentiated adipocytes. While all the lncRNAs analyzed were increased in mature adipocytes, NEAT1 expression was increased 7-fold in mature adipocytes, far above the increase we saw in other lncRNAs. These

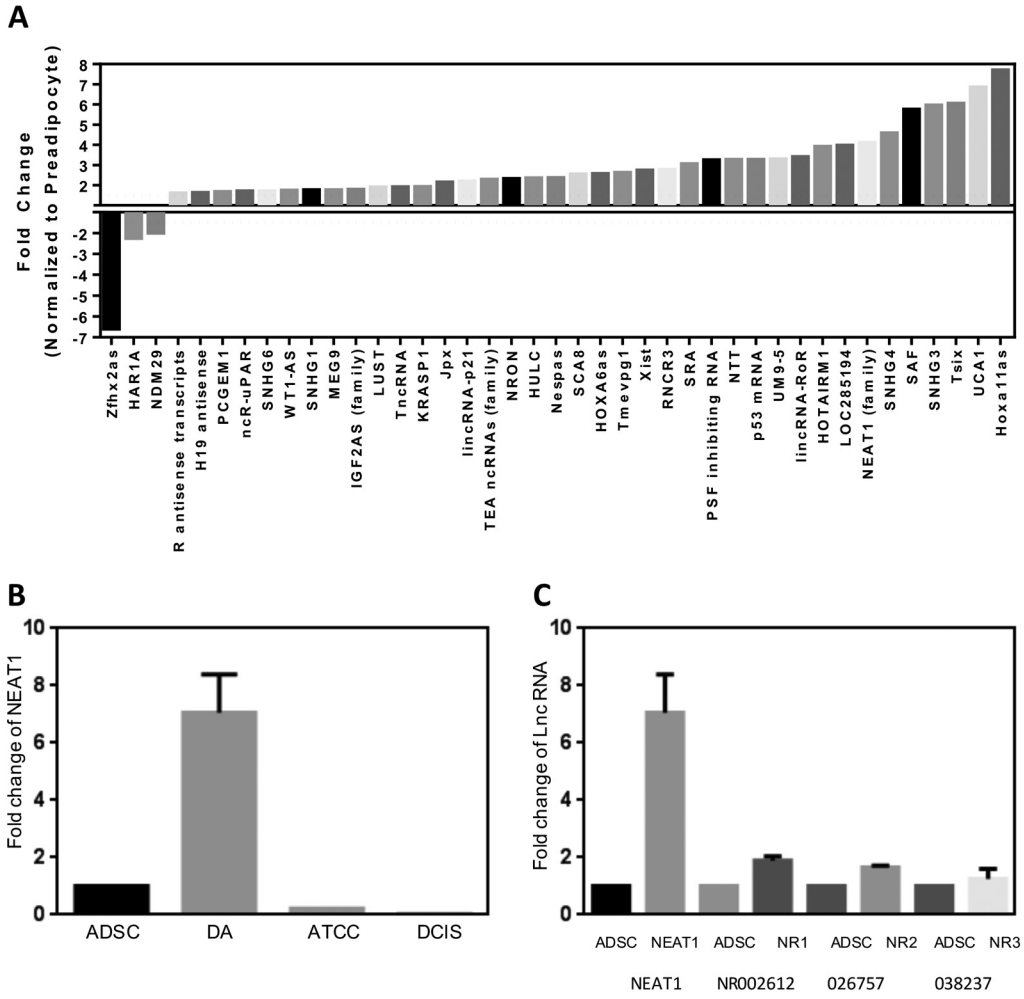

Gene	Fold Change
Zfhx2as	***-6.5738381***
HAR1A	***-2.2295243***
NDM29	***-1.9816964***
PR antisense transcripts	1.5946768
H19 antisense	1.6169377
PCGEM1	1.662396
ncR-uPAR	1.6973264
SNHG6	1.6973264
WT1-AS	1.7329909
SNHG1	1.7571825
MEG9	1.7571825
IGF2AS (family)	1.7694047
LUST	1.8833016
TncRNA	1.896401
KRASP1	1.9095915
Jpx	2.133562
lincRNA-p21	2.1783927
TEA ncRNAs (family)	2.2708998
NRON	2.3026004
HULC	2.3347435
Nespas	2.3509829
SCA8	2.5372472
HOXA6as	2.5548951
Tmevpg1	2.6085789
Xist	2.7193542
RNCR3	2.7573149
SRA	3.0382994
PSF inhibiting RNA	3.2338753
NTT	3.2563687
p53 mRNA	3.2563687
UM9-5	3.2790186
lincRNA-RoR	3.3946529
HOTAIRM1	3.8994322
LOC285194	3.9538662
NEAT1 (family)	4.093299
SNHG4	4.5733904
SAF	5.7488129
SNHG3	5.9515443
Tsix	6.0346248
UCA1	6.8365291
Hoxa11as	7.6914951

FIG 2 Differential expression of lncRNAs in adipocytes compared to preadipocytes. (A) A 96-well-based human Lnc profiler qPCR array consisting of 90 different lncRNAs, along with 5 housekeeping genes and one negative control, was used to screen adipocytes. The results for the genes that are either upregulated or downregulated by at least 1.5-fold are listed in the table. (B) Expression levels of NEAT1 in preadipocytes (ADSCs) and differentiated adipocytes (DA) compared to ATCC (human lung fibroblasts) and DCIS (MCF10DCIS). (C) Comparative analysis of lncRNA identified by NCBI reference number (NR). The data represent means and SE ($n = 3$).

data confirm the results of our noncoding RNA array and demonstrate that NEAT1 is upregulated in human adipocytes during adipogenesis.

miR-140 can regulate lncRNA-NEAT1. As miRNAs can shuttle back to the nucleus and regulate nuclear mRNAs and noncoding RNAs (28), we hypothesized that miR-140 is imported into the nucleus and regulates the nuclear NEAT1. Using the RNAhybrid algorithm, we identified two putative miR-140 binding sites in NEAT1 at bp 974 to 998 and bp 2370 to 2403 (Fig. 3A). To determine whether these predicted miR-140 binding sites were involved in NEAT1 regulation, we constructed pGL3 luciferase reporter vectors containing the potential miR-140 binding sites found within NEAT1 and performed a luciferase reporter assay. HEK293T cells were cotransfected with miR-140 overexpression vector, the pGL3 NEAT1 luciferase vector construct, and pRL-TK *Renilla* luciferase vector. As shown in Fig. 3B and C, there was increased luciferase activity in cells transfected with the reporter containing miR-140 binding site 1 (BS1) (bp 974 to 998) but not binding site 2 (BS2) (bp 2370 to 2403). To further confirm that binding site 1 is necessary for miR-140 to regulate NEAT1 activity, we constructed a pGL3 luciferase reporter containing a mutated version of binding site 1. Cells transfected with the mutated binding site 1 vector had abrogated luciferase activity compared to cells transfected with the WT binding site 1 vector (Fig. 3D). To verify that miR-140 directly binds to NEAT1, we employed direct affinity purification. We designed a biotinylated miR-140 construct that binds to streptavidin beads, allowing the purification of the RNA that physically interacts with miR-140. After transfecting the biotinylated miR-140 construct into 3T3-L1 mouse preadipocytes, we lysed the transfected cells and incubated the whole-cell lysates with biotin-binding streptavidin magnetic beads to isolate the biotinylated miR-140 complex. Using qRT-PCR, we determined the enrichment of specific RNA bound by the biotinylated miR-140 construct normalized to β-actin RNA. NEAT1 RNA was significantly enriched by pulldown with biotin–miR-140 compared to cells transfected with control scrambled RNA (Fig. 3E). As a positive control, we analyzed enrichment of HDAC4, a known target of miR-140 (37). As expected, *hdac4*

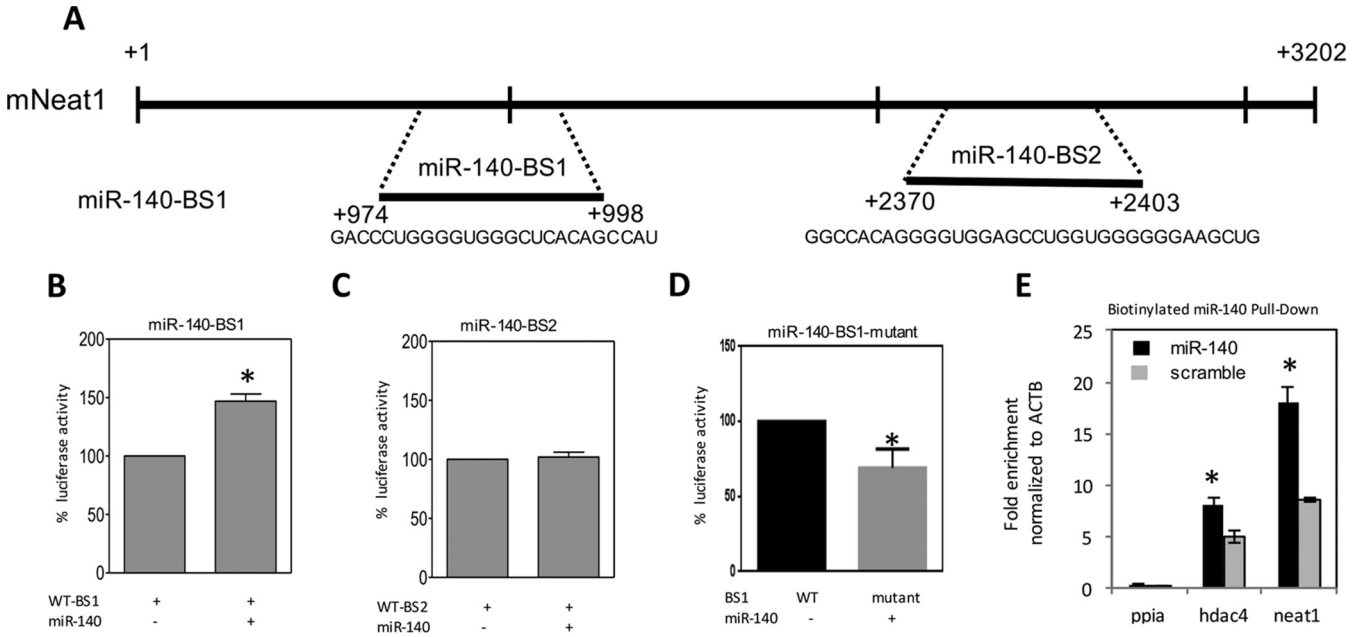

FIG 3 The miR-140 binding sites within mouse NEAT1 (mNeat1) were identified using RNAhybrid 2.2. (A) Target binding sites of miR-140 (BS1 and BS2) within NEAT1. (B) Luciferase reporter assays were performed and confirmed that ectopic expression of miR-140 increased the activity of the BS1 reporter. (C) Ectopic expression of miR-140 has no impact on BS2. (D) Mutation of BS1 inhibited miR-140 induction of luciferase activity. (E) Biotin-labeled miR-140 pulldown demonstrated binding of miR-140 to NEAT1. ACTB, β-actin. The data represent means and SE ($n = 3$). *, $P < 0.05$.

mRNA was highly enriched by biotin–miR-140. In contrast, PPIA mRNA, which is not a target for miR-140, was not enriched by biotin–miR-140 (Fig. 3E), suggesting the specificity of the interaction of miR-140 and NEAT1.

miR-140 binding leads to enhanced NEAT1 expression. As we identified direct binding of miR-140 to NEAT1, we next wanted to examine whether miR-140 binding impacts NEAT1 expression. The most common miRNA function is targeting mRNA transcripts for degradation. Conversely, the best-characterized role of lncRNA-miRNA binding is the inhibition of miRNA activity by competitive-endogenous lncRNA (26). While miRNAs are best known for their cytoplasmic functions, several studies have shown that miRNAs, as well as RISC proteins, are imported into the nucleus and are able to degrade nuclear RNA molecules (6). This is a mechanism by which miRNAs can decrease the expression of both mRNA and lncRNA. Some miRNAs have also been shown to bind to DNA and activate gene transcription (7), while others are able to stabilize mRNA by preventing binding of degradative proteins (9). As both miR-140 and NEAT1 are upregulated in adipogenesis, we predicted that miR-140 binding may positively regulate NEAT1 expression. We first examined NEAT1 expression levels in primary human adipocyte-derived stem cells, as well as cells isolated from lung and mammary tissues of WT and miR-140 KO mice. Using qRT-PCR, we found that NEAT1 expression was dramatically decreased in all miR-140 KO primary cells examined (Fig. 4A). We then overexpressed miR-140 in 3T3-L1 preadipocytes and human lung fibroblasts and observed an increase of NEAT1 expression in both cell lines (Fig. 4B). Because NEAT1 expression is restricted to the nucleus, we used immunofluorescence staining for miR-140 and NEAT1 to study their cellular localization and to determine if they colocalize in the nucleus. In WT primary adipocyte-derived stem cells and 3T3-L1 preadipocytes, miR-140 was expressed in both the cytoplasm and nucleus, with NEAT1 restricted to the nucleus (Fig. 4C and D). Immunofluorescence staining in primary miR-140 KO adipocyte-derived stem cells demonstrated the complete abrogation of miR-140 expression in KO mice compared to WT adipocyte-derived stem cells, which corresponded to a decrease in NEAT1 expression (Fig. 4C). When we overexpressed miR-140 in 3T3-L1 preadipocytes, we also saw an increase in NEAT1 staining (Fig. 4D). To investigate if miR-140 may impact NEAT1 stability, we performed an actinomycin D RNA stability assay. Previous reports have demonstrated that mouse NEAT1 has a half-life of between 15 and 30 min (38). Using these previously reported time points, we observed degradation of NEAT1 in control cells, while overexpression of miR-140 increased NEAT1 stability with no degradation seen within the studied time (Fig. 4E). Overall, these data indicate that miR-140 binds to NEAT1 in the nucleus and enhances NEAT1 stability.

miR-140 activation of NEAT1 is required for adipogenesis. Finally, we investigated the functional role of the miR-140/NEAT1 signaling pathway in adipogenesis. Adipocyte-derived stem cells are able to proliferate and self-renew, maintaining a pool of committed mature adipocyte progenitor cells. We previously found that miR-140 regulates breast cancer stem cell self-renewal through degradation of stem cell factors SOX2 and SOX9 (17). Therefore, we used a sphere formation assay to investigate whether miR-140 regulates self-renewal in adipocyte-derived stem cells, as well. We plated primary WT and miR-140 KO adipocyte-derived stem cells on polyhema-coated, nonadherent plates. Under these conditions, cells capable of self-renewal form spheroids while others die from anoikis. The number of spheres formed is used to determine the self-renewal ability of the cells. miR-140 KO adipocyte-derived stem cells formed twice the number of spheres as WT adipocyte-derived stem cells, consistent with

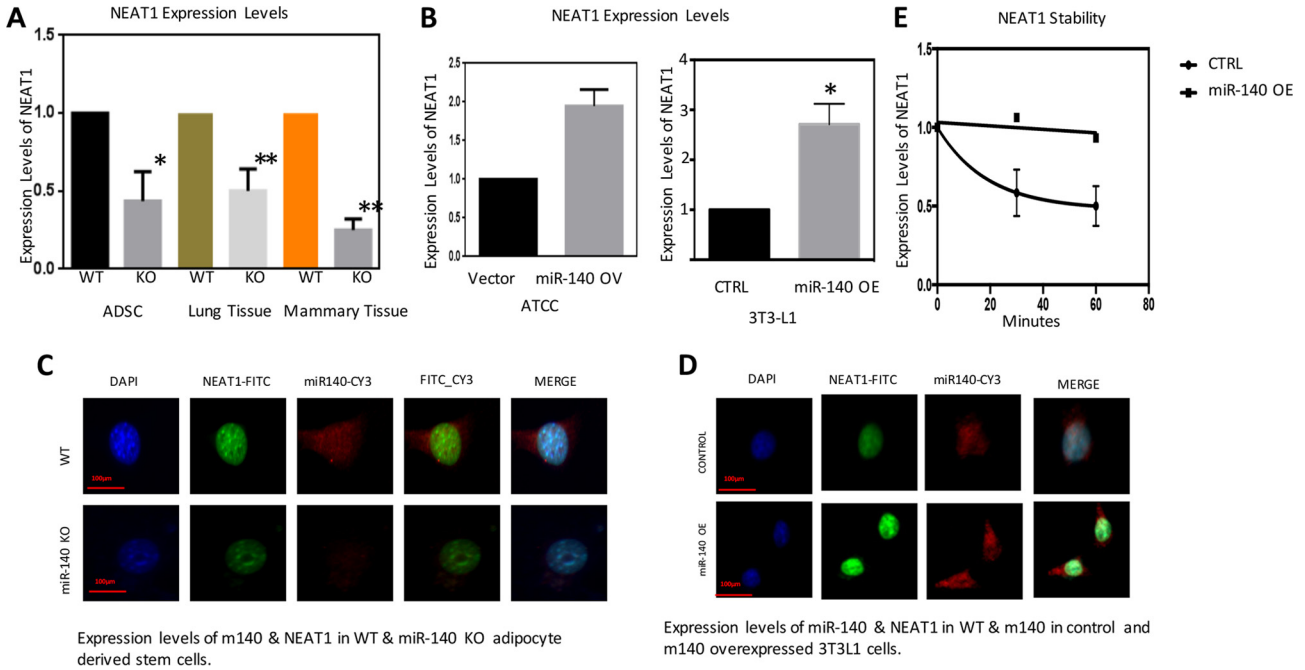

FIG 4 Expression levels of NEAT1 by RT-PCR analysis and validation of miR-140 downregulation in preadipocytes. (A) Comparison of NEAT1 expression levels in WT and miR-140 KO adipocyte-derived stem cells and lung and mammary tissues. (B) NEAT1 expression is increased by overexpression (OE) of miR-140 in ATCC (human lung fibroblasts) and 3T3-L1 (preadipocytes) cells. (C) Adipocyte-derived stem cells obtained from WT and miR-140 KO mice were stained with NEAT1 probe and antidigoxigenin (anti-DIG) antibodies (for miR-140) and visualized by fluorescence. Shown are expression levels of m140 and NEAT1 in WT and miR-140 KO adipocyte-derived stem cells. (D) 3T3-L1 cells were transfected with either pCAG-GFP (control vector) or miR-140 overexpression vector. The transfected cells were fixed and analyzed for changes in the expression levels of NEAT1 through *in situ* hybridization of NEAT1 and miR-140 probes. *In situ* hybridization of miR-140 (5′ DIG tagged; identified using anti-DIG Cy3-conjugated antibody) and NEAT1 probes (FITC conjugated). Shown are expression levels of miR-140 and NEAT1 in WT and miR-140 (m140) in control and miR-140-overexpressing 3T3-L1 cells. (E) Demonstration of NEAT1 stability in miR-140-overexpressing 3T3-L1 cells. The data represent means and SE ($n = 3$). *, $P < 0.05$; **, $P < 0.01$.

our previous functional studies of miR-140 (16, 17). Moreover, the spheres formed by KO cells were larger and more robust, indicating the greater proliferative capabilities of the KO cells (Fig. 5A and B). Using qRT-PCR, we examined the expression change of the key stem cell regulatory factors octamer-binding transcription factor 4 (OCT-4), SOX2, and SOX9. We found that OCT-4 was much more highly expressed in miR-140 KO spheres than in the WT (Fig. 5C), while SOX2 and SOX9 levels were unchanged (data not shown). This indicates that OCT-4 is an important self-renewal regulator in miR-140 KO cells. We next wanted to determine if the lack of miR-140 activation of NEAT1 inhibits adipogenesis in miR-140 KO cells (Fig. 1). We overexpressed NEAT1 in miR-140 KO primary adipocyte-derived stem cells (Fig. 5E) and found significant upregulation of both CEBPα and PPARγ (Fig. 5G and H). Oil Red O staining revealed a remarkable increase in the number of mature adipocytes when NEAT1 was overexpressed in miR-140 KO adipocyte-derived stem cells (Fig. 5D and F). These data show that the inhibition of self-renewal by miR-140 previously reported in breast cancer stem cells also occurs in adipocyte-derived stem cells and that activation of NEAT1 is a critical role of miR-140 in adipogenesis.

DISCUSSION

Previous studies have shown that cytoplasmic miR-140 targets SOX2 and SOX9 for degradation, two factors important in both chondrogenesis and stemness, self-renewal and pluripotent ability (15, 16). miR-140 was recently demonstrated to be activated by BMP-4 and to induce commitment to the adipogenic lineage through the targeted degradation of OSTM1 (19). Profiling of the global mouse adipocyte noncoding transcriptome by Sun et al. found that lncRNA NEAT1 is one of the most upregulated long-noncoding RNAs in adipogenesis (13). Here, we found that miR-140 localizes to the nucleus and increases NEAT1 expression. Moreover, we found that this relationship is critical for adipogenesis, defining new functions of both miR-140 and NEAT1.

Through the use of primary adipocyte-derived stem cells isolated from miR-140 KO mice, we observed that miR-140 KO adipocyte-derived stem cells have abrogated adipogenic ability compared to the WT, as shown through decreased Oil Red O staining and PPARγ and C/EBPα expression. Profiling of mature mouse adipocytes confirmed that NEAT1 is upregulated in mature mouse adipocytes (13) and also increased in mature human adipocytes.

NEAT1 expression is significantly decreased in miR-140 KO adipocyte-derived stem cells and was rescued upon overexpression of miR-140. We observed that miR-140 localizes to the nucleus, and using a biotinylated miR-140 probe, we demonstrated a physical interaction between miR-140 and NEAT1 that increases NEAT1 stability and expression. These data demonstrate a positive signaling relationship between miR-140 and NEAT1.

Finally, we demonstrated that positive regulation of NEAT1 by miR-140 is necessary for adipogenesis. Reexpression of NEAT1 in miR-140 KO adipocyte-derived stem cells was sufficient to rescue the adipogenic phenotype, showing that lower expression of

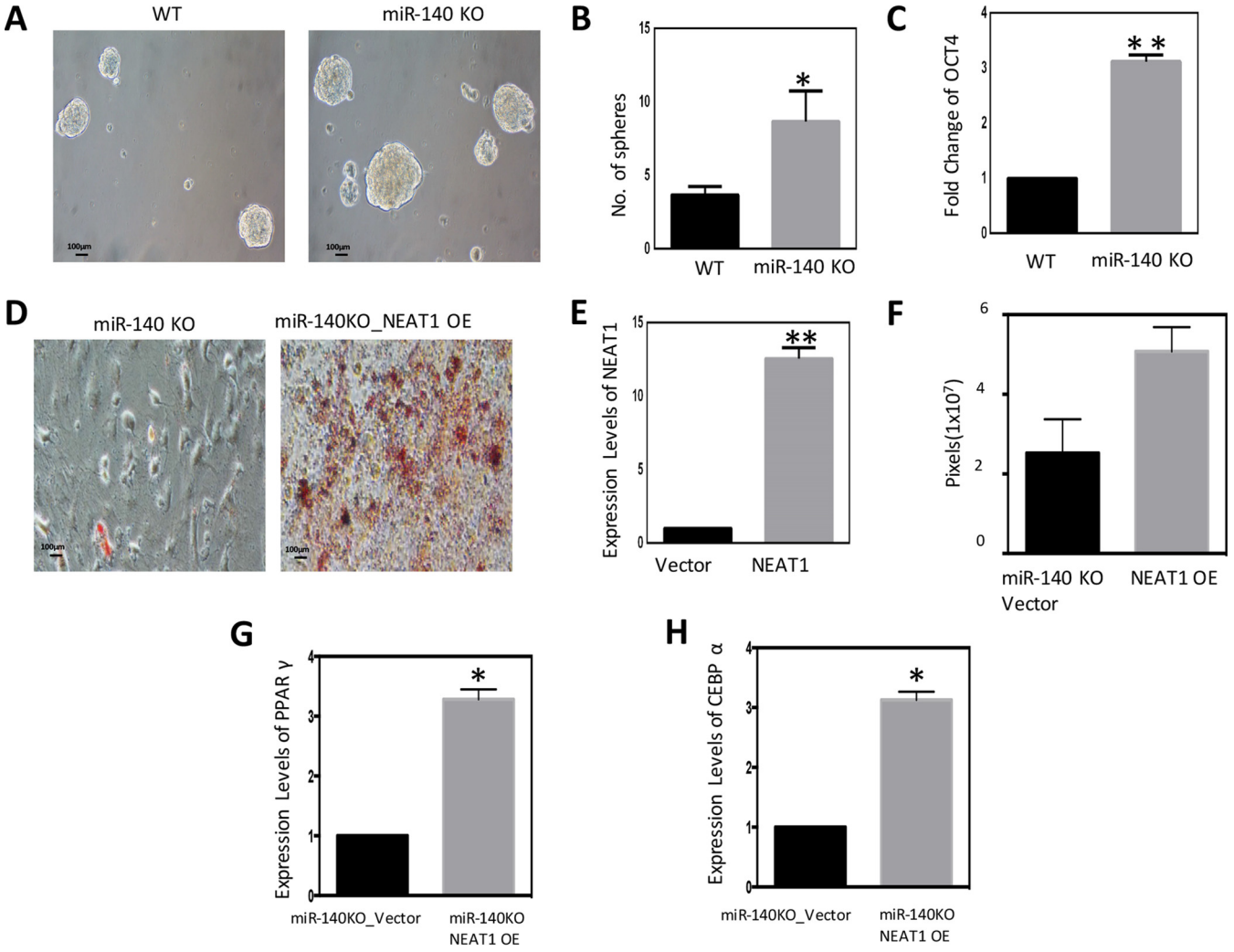

FIG 5 Effects of NEAT1 overexpression on the process of differentiation. (A) Demonstration of numbers and sizes of spheres with adipocyte-derived stem cells of WT and miR-140 KO mice. (B) Quantification of spheres measuring more than 100 μm. (C) Fold change of OCT-4 levels in the spheres of WT and miR-140 KO cells by RT-PCR. (D) NEAT1 overexpression in miR-140 KO adipocyte-derived stem cells resulted in an increase in differentiation. (E) Confirmation of NEAT1 overexpression by RT-PCR. (F) Representation of the amount of Oil Red dye in lipid droplets by ImageJ analysis. (G and H) Expression levels of CEBP/α and PPARγ in vector (control) and NEAT1-overexpressing miR-140 KO adipocyte-derived stem cells. The data represent means and SE ($n = 3$). *, $P < 0.05$; **, $P < 0.01$. Scale bars (A and D), 100 μm.

NEAT1 in miR-140 KO adipocyte-derived stem cells inhibits their adipogenic abilities.

While the structural role of NEAT1 in paraspeckles has been well characterized, little is known about the regulation of NEAT1 or its roles outside paraspeckle formation. The novel relationship between miR-140 and NEAT1 we have identified is critical for adipogenesis and is an exciting discovery that defines a new role for miR-140 in the regulation and functionof NEAT1.

FUNDING INFORMATION

NIH provided funding to Qun Zhou under grant numbers CA157779A1 and CA163820A1. ACS provided funding to Qun Zhou under grant number RSG-12-006-01-CNE. NIH provided funding to Hiroshi Asahara under grant numbers AR050631 and AR065379. AMED-CREST provided funding to Hiroshi Asahara. JSPS provided funding to Hiroshi Asahara.

REFERENCES

1. **Ogden CL, Carroll MD, Kit BK, Flegal KM.** 2014. Prevalence of childhood and adult obesity in the United States, 2011–2012. JAMA **311:**806–814. http://dx.doi.org/10.1001/jama.2014.732.
2. **Ewertz M, Jensen MB, Gunnarsdottir KA, Hojris I, Jakobsen EH, Nielsen D, Stenbygaard LE, Tange UB, Cold S.** 2011. Effect of obesity on prognosis after early-stage breast cancer. J Clin Oncol **29:**25–31. http://dx.doi.org/10.1200/JCO.2010.29.7614.
3. **Protani M, Coory M, Martin JH.** 2010. Effect of obesity on survival of women with breast cancer: systematic review and meta-analysis. Breast Cancer Res Treat **123:**627–635. http://dx.doi.org/10.1007/s10549-010-0990-0.
4. **Cristancho AG, Lazar MA.** 2011. Forming functional fat: a growing understanding of adipocyte differentiation. Nat Rev Mol Cell Biol **12:**722–734. http://dx.doi.org/10.1038/nrm3198.
5. **Dirat B, Bochet L, Dabek M, Daviaud D, Dauvillier S, Majed B, Wang Y-Y, Meulle A, Salles B, Le Gonidec S, Garrido I, Escourrou G, Valet P, Muller C.** 2011. Cancer-associated adipocytes exhibit an activated phenotype and contribute to breast cancer invasion. Cancer Res **71:**2455–2465. http://dx.doi.org/10.1158/0008-5472.CAN-10-3323.
6. **Leucci E, Patella F, Waage J, Holmstrøm K, Lindow M, Porse B, Kauppinen S, Lund AH.** 2013. microRNA-9 targets the long non-coding RNA MALAT1 for degradation in the nucleus. Sci Rep **3:**2535. http://dx.doi.org/10.1038/srep02535.
7. **Li L-C, Okino ST, Zhao H, Pookot D, Place RF, Urakami S, Enokida H, Dahiya R.** 2006. Small dsRNAs induce transcriptional activation in hu-

man cells. Proc Natl Acad Sci U S A **103:**17337–17342. http://dx.doi.org/10.1073/pnas.0607015103.
8. **Portnoy V, Huang V, Place RF, Li L-C.** 2011. Small RNA and transcriptional upregulation. Wiley Interdiscip Rev RNA **2:**748–760. http://dx.doi.org/10.1002/wrna.90.
9. **Ma F, Liu X, Li D, Wang P, Li N, Lu L, Cao X.** 2010. MicroRNA-466l upregulates IL-10 expression in TLR-triggered macrophages by antagonizing RNA-binding protein tristetraprolin-mediated IL-10 mRNA degradation. J Immunol **184:**6053–6059. http://dx.doi.org/10.4049/jimmunol.0902308.
10. **Garzon R, Calin GA, Croce CM.** 2009. MicroRNAs in Cancer. Annu Rev Med **60:**167–179. http://dx.doi.org/10.1146/annurev.med.59.053006.104707.
11. **Karbiener M, Pisani DF, Frontini A, Oberreiter LM, Lang E, Vegiopoulos A, Mössenböck K, Bernhardt GA, Mayr T, Hildner F, Grillari J, Ailhaud G, Herzig S, Cinti S, Amri E-Z, Scheideler M.** 2014. MicroRNA-26 family is required for human adipogenesis and drives characteristics of brown adipocytes. Stem Cells **32:**1578–1590. http://dx.doi.org/10.1002/stem.1603.
12. **Walden TB, Timmons JA, Keller P, Nedergaard J, Cannon B.** 2009. Distinct expression of muscle-specific microRNAs (myomirs) in brown adipocytes. J Cell Physiol **218:**444–449. http://dx.doi.org/10.1002/jcp.21621.
13. **Sun L, Goff LA, Trapnell C, Alexander R, Lo KA, Hacisuleyman E, Sauvageau M, Tazon-Vega B, Kelley DR, Hendrickson DG, Yuan B, Kellis M, Lodish HF, Rinn JL.** 2013. Long noncoding RNAs regulate adipogenesis. Proc Natl Acad Sci U S A **110:**3387–3392. http://dx.doi.org/10.1073/pnas.1222643110.
14. **Trajkovski M, Ahmed K, Esau CC, Stoffel M.** 2012. MyomiR-133 regulates brown fat differentiation through Prdm16. Nat Cell Biol **14:**1330–1335. http://dx.doi.org/10.1038/ncb2612.
15. **Miyaki S, Sato T, Inoue A, Otsuki S, Ito Y, Yokoyama S, Kato Y, Takemoto F, Nakasa T, Yamashita S, Takada S, Lotz MK, Ueno-Kudo H, Asahara H.** 2010. MicroRNA-140 plays dual roles in both cartilage development and homeostasis. Genes Dev **24:**1173–1185. http://dx.doi.org/10.1101/gad.1915510.
16. **Li Q, Eades G, Yao Y, Zhang Y, Zhou Q.** 2014. Characterization of a stem-like subpopulation in basal-like ductal carcinoma in situ (DCIS) lesions. J Biol Chem **289:**1303–1312. http://dx.doi.org/10.1074/jbc.M113.502278.
17. **Li Q, Yao Y, Eades G, Liu Z, Zhang Y, Zhou Q.** 2014. Downregulation of miR-140 promotes cancer stem cell formation in basal-like early stage breast cancer. Oncogene **33:**2589–2600. http://dx.doi.org/10.1038/onc.2013.226.
18. **Zhang Y, Eades G, Yao Y, Li Q, Zhou Q.** 2012. Estrogen receptor α signaling regulates breast tumor-initiating cells by down-regulating miR-140 which targets the transcription factor SOX2. J Biol Chem **287:**41514–41522. http://dx.doi.org/10.1074/jbc.M112.404871.
19. **Liu Y, Zhang Z-C, Qian S-W, Zhang Y-Y, Huang H-Y, Tang Y, Guo L, Li X, Tang Q-Q.** 2013. MicroRNA-140 promotes adipocyte lineage commitment of C3H10T1/2 pluripotent stem cells via targeting osteopetrosis-associated transmembrane protein 1. J Biol Chem **288:**8222–8230. http://dx.doi.org/10.1074/jbc.M112.426163.
20. **Naganuma T, Hirose T.** 2013. Paraspeckle formation during the biogenesis of long non-coding RNAs. RNA Biol **10:**456–461. http://dx.doi.org/10.4161/rna.23547.
21. **Standaert L, Adriaens C, Radaelli E, Van Keymeulen A, Blanpain C, Hirose T, Nakagawa S, Marine J-C.** 2014. The long noncoding RNA Neat1 is required for mammary gland development and lactation. RNA **20:**1844–1849. http://dx.doi.org/10.1261/rna.047332.114.
22. **Chen L-L, Carmichael GG.** 2009. Altered nuclear retention of mRNAs containing inverted repeats in human embryonic stem cells: functional role of a nuclear noncoding RNA. Mol Cell **35:**467–478. http://dx.doi.org/10.1016/j.molcel.2009.06.027.
23. **West JA, Davis CP, Sunwoo H, Simon MD, Sadreyev RI, Wang PI, Tolstorukov MY, Kingston RE.** 2014. The long noncoding RNAs NEAT1 and MALAT1 bind active chromatin sites. Mol Cell **55:**791–802. http://dx.doi.org/10.1016/j.molcel.2014.07.012.
24. **Chakravarty D, Sboner A, Nair SS, Giannopoulou E, Li R, Hennig S, Mosquera JM, Pauwels J, Park K, Kossai M, MacDonald TY, Fontugne J, Erho N, Vergara IA, Ghadessi M, Davicioni E, Jenkins RB, Palanisamy N, Chen Z, Nakagawa S, Hirose T, Bander NH, Beltran H, Fox AH, Elemento O, Rubin MA.** 2014. The oestrogen receptor alpha-regulated lncRNA NEAT1 is a critical modulator of prostate cancer. Nat Commun **5:**5383. http://dx.doi.org/10.1038/ncomms6383.
25. **Zhou X, Gao Q, Wang J, Zhang X, Liu K, Duan Z.** 2014. Linc-RNA-RoR acts as a "sponge" against mediation of the differentiation of endometrial cancer stem cells by microRNA-145. Gynecol Oncol **133:**333–339. http://dx.doi.org/10.1016/j.ygyno.2014.02.033.
26. **Eades G, Wolfson B, Zhang Y, Li Q, Yao Y, Zhou Q.** 2015. lincRNA-RoR and miR-145 regulate invasion in triple-negative breast cancer via targeting ARF6. Mol Cancer Res **13:**330–338. http://dx.doi.org/10.1158/1541-7786.MCR-14-0251.
27. **Cheng E-C, Lin H.** 2013. Repressing the repressor: a lincRNA as a microRNA sponge in embryonic stem cell self-renewal. Dev Cell **25:**1–2. http://dx.doi.org/10.1016/j.devcel.2013.03.020.
28. **Liang H, Zhang J, Zen K, Zhang C-Y, Chen X.** 2013. Nuclear microRNAs and their unconventional role in regulating non-coding RNAs. Protein Cell **4:**325–330. http://dx.doi.org/10.1007/s13238-013-3001-5.
29. **Gernapudi R, Yao Y, Zhang Y, Wolfson B, Roy S, Duru N, Eades G, Yang P, Zhou Q.** 2015. Targeting exosomes from preadipocytes inhibits preadipocyte to cancer stem cell signaling in early-stage breast cancer. Breast Cancer Res Treat **150:**685–695. http://dx.doi.org/10.1007/s10549-015-3326-2.
30. **Li Q, Xia J, Yao Y, Gong D-W, Shi H, Zhou Q.** 2013. Sulforaphane inhibits mammary adipogenesis by targeting adipose mesenchymal stem cells. Breast Cancer Res Treat **141:**317–324. http://dx.doi.org/10.1007/s10549-013-2672-1.
31. **Matsumoto T, Kano K, Kondo D, Fukuda N, Iribe Y, Tanaka N, Matsubara Y, Sakuma T, Satomi A, Otaki M, Ryu J, Mugishima H.** 2008. Mature adipocyte-derived dedifferentiated fat cells exhibit multilineage potential. J Cell Physiol **215:**210–222. http://dx.doi.org/10.1002/jcp.21304.
32. **Yin QF, Hu SB, Xu YF, Yang L, Carmichael GG, Chen LL.** 2015. SnoVectors for nuclear expression of RNA. Nucleic Acids Res **43:**e5. http://dx.doi.org/10.1093/nar/gku1050.
33. **Orom UA, Lund AH.** 2007. Isolation of microRNA targets using biotinylated synthetic microRNAs. Methods **43:**162–165. http://dx.doi.org/10.1016/j.ymeth.2007.04.007.
34. **de Planell-Saguer M, Rodicio MC, Mourelatos Z.** 2010. Rapid in situ codetection of noncoding RNAs and proteins in cells and formalin-fixed paraffin-embedded tissue sections without protease treatment. Nat Protoc **5:**1061–1073. http://dx.doi.org/10.1038/nprot.2010.62.
35. **Eades G, Yao Y, Yang M, Zhang Y, Chumsri S, Zhou Q.** 2011. miR-200a regulates SIRT1 expression and epithelial to mesenchymal transition (EMT)-like transformation in mammary epithelial cells. J Biol Chem **286:**25992–26002. http://dx.doi.org/10.1074/jbc.M111.229401.
36. **Moreno-Navarrete JM, Fernández-Real JM.** 2011. Adipocyte differentiation, p 17–38. *In* Symonds ME (ed), Adipose tissue biology. Springer, New York, NY.
37. **Tuddenham L, Wheeler G, Ntounia-Fousara S, Waters J, Hajihosseini MK, Clark I, Dalmay T.** 2006. The cartilage specific microRNA-140 targets histone deacetylase 4 in mouse cells. FEBS Lett **580:**4214–4217. http://dx.doi.org/10.1016/j.febslet.2006.06.080.
38. **Clark MB, Johnston RL, Inostroza-Ponta M, Fox AH, Fortini E, Moscato P, Dinger ME, Mattick JS.** 2012. Genome-wide analysis of long noncoding RNA stability. Genome Res **22:**885–898. http://dx.doi.org/10.1101/gr.131037.111.
39. **Rehmsmeier M, Steffen P, Hochsmann M, Giegerich R.** 2004. Fast and effective prediction of microRNA/target duplexes. RNA **10:**1507–1517. http://dx.doi.org/10.1261/rna.5248604.